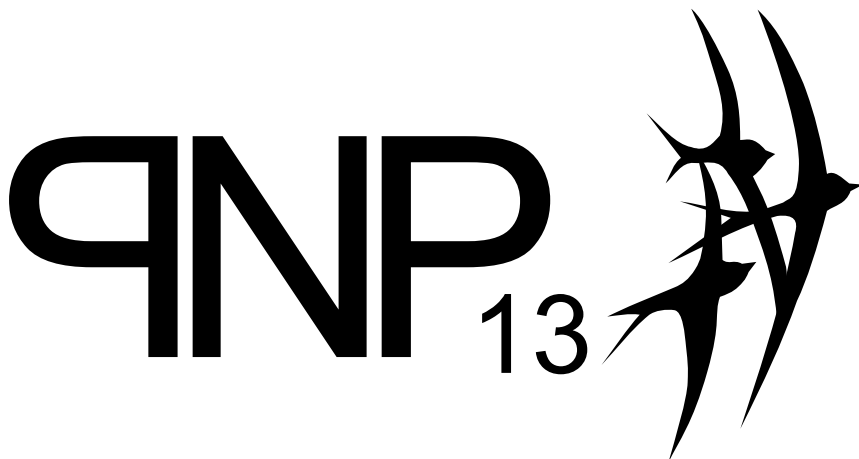


Russian Academy of Sciences
Institute of Problems of Chemical Physics RAS
Joint Institute for High Temperatures RAS



XIII International Conference on
Physics of Non-Ideal Plasmas
September 13 — 18, 2009, Chernogolovka, Russia

Poster session S8

Chernogolovka 2009

Contents

1	Statistical physics and mathematical modeling of strongly coupled Coulomb systems	7
1.1	Mathematical simulation of kinetic processes in the non-ideal nuclear-excited dust plasma of the noble gases <i>Budnik A.P., Deputatova L.V., Fortov V.E., Kosarev V.A., Rykov V.A., Vladimirov V.I., JIHT RAS</i>	7
1.3	Calculation of canonical properties and excited states by path integral numerical methods <i>Vorontsov-Velyaminov P.N., Voznesenskiy M.A., Polyakov E.A., Lyubartsev A.P., SPbSU, SU</i>	8
1.4	Investigation formation of charge and of energy spectra of multiply charged ions, generated under the action of laser radiation on the surface of two-element targets Tm_2O_3 , Yb_2O_3 and Eu_2O_3 <i>Khaydarov R., Berdierov G., IAPh-Tashkent</i>	9
1.7	Quantum Potential including Diffraction and Exchange Effects <i>Dufty J.W., Dutta S., Bonitz M., Filinov A., CAU, U. Florida</i>	10
1.9	Semi-Classical Model of Strongly Correlated Coulomb Systems in Weak Magnetic Field <i>Ciftja O., PVAMU</i>	10
1.11	Interfacial Properties of the Strongly Coupled Imidazolium Ionic Liquids: a Molecular Dynamics Study <i>Kislenko S.A., Samoylov I.S., Amirov R.H., JIHT RAS</i>	11
1.13	Specific Features of Spallation Processes in Polymethylmetacrylate under High Strain Rate <i>Krasyuk I.K., Geraskin A.A., Khishchenko K.V., Pashinin P.P., Semenov A.Y., Vovchenko V.I., GPI, IEP UB RAS, JIHT RAS</i>	12
1.14	Transition of Electromagnetic Wave Through a Warm Overdense Plasma <i>Rajaei L., Mirabotalebi S., AU, QOMU</i>	13
1.15	Coulomb systems' modeling under consideration of finite instrumental resolution scales <i>Minkova N.R., TSU</i>	13
1.16	Ionization cross section for strongly coupled hydrogen plasma with arbitrary ionization degree <i>Baimbetov F.B., Kudyshev Z.A., IETP KazNU</i>	14
1.17	Modeling of Dielectrics Bombardment with Swift Heavy Ions <i>Ivanov D.S., Osmani O., Rethfeld B., TUKL</i>	15

1.23	Formation of the globular defects in fluorite-like ionic crystals <i>Yakub L.N., Yakub E.S., OSAR, OSEU</i>	16
2	Equilibrium properties and equation of state of dense plasmas	18
2.2	Phase shifts and the second virial coefficient for a partially ionized Hydrogen plasma <i>Ramazanov T.S., Omarbakiyeva Y.A., Röpke G., IETP KazNU, U. Rostock</i>	18
2.3	Electrical resistivity in warm dense plasmas beyond the average-atom model <i>Pain J.C., Dejonghe G., CEA</i>	19
2.4	Modeling of Thermodynamic Properties of Dense Multicharged-Ion Plasmas Based on the Chemical-Picture Approach <i>Shadrin A.A., Loboda P.A., Popova V.V., RFNC-VNIITF</i>	19
2.8	Dielectric catastrophe and insulator-metal transition in AlH ₃ . <i>Khrapak A.G., Molodets A.M., Shakh-ray D.V., Fortov V.E., IPCP RAS, JIHT RAS</i>	20
2.10	Use of Pulsed Radiography for Investigation of Equation of States of Substances at Megabar Pressures <i>Egorov N.I., Boriskov G.V., Bykov A.I., Kuropatkin Yu.P., Luk'yanov N.B., Mironenko V.D., Pavlov V.N., RFNC-VNIIEF</i>	21
2.11	Multiphase equation of state for iron at high pressures and temperatures <i>Khishchenko K.V., JIHT RAS</i>	22
2.14	Semiempirical equations of state for metals based on Thomas–Fermi model <i>Shemyakin O.P., Khishchenko K.V., JIHT RAS</i>	22
2.15	Thermodynamic Properties of Gaseous Plasmas in the Zero-Temperature Limit <i>Iosilevskiy I.L. JIHT RAS</i>	23
3	Kinetics, transport and optical properties of dense Coulomb systems	25
3.2	Magnetotransport properties of dense plasmas <i>Reinholz H., Adams J., Röpke G., Redmer R., Shilkin N.S., Mintsev V.B., Gryaznov V.K., IPCP RAS, U. Rostock, UWA</i>	25
3.4	The calculations of transport coefficients of noble gases under high pressures <i>Apfelbaum E.M., JIHT RAS</i>	26

3.6	On the replacement of collisional recombination mechanism in nonideal plasma. <i>Lankin A.V., MIPT</i>	27
3.8	Pressure Broadening of Spectral Lines in Dense Lithium Plasmas <i>Lorenzen S., Wierling A., Reinholz H., Röpke G., U. Rostock</i>	27
3.9	Radiation Hydrodynamics of Laser-induced Plasmas using Dynamic Collision Frequencies <i>Sperling P., Wierling A., Röpke G., Winkel M., U. Rostock</i>	28
3.11	Quantum kinetic approach to time-resolved photoionization of multi-electron atoms <i>Bauch S., Hochstuhl D., Balzer K., Bonitz M., CAU</i>	30
3.13	Atomic Database Spectr-W ³ for Plasma Spectroscopy and Other Applications. Current Status and Perspectives <i>Loboda P.A., Gagarin S.V., Kozlov A.I., Morozov S.V., Popova V.V., Vanina I.A., Faenov A.Ya., Magunov A.I., Pikuz T.A., Skobelev I.Yu., Urnov A.M., Vainshtein L.A., FIAN, JIHT RAS, RFNC-VNIITF</i>	31
3.15	The modeling of the continuous absorption spectra of the dense hydrogen plasma on the base of the cut-off Coulomb potential <i>Sakan N.M., Mihajlov A.A., Ignjatovic Lj.M., Sreckovic V.A., IoP</i>	32
3.17	Interparticle interactions effect on behavior of caloric equation of state for plasma of dense metals vapor <i>Shumikhin A.S., Khomkin A.L., JIHT RAS</i>	32
3.19	Transport coefficients in dense plasmas including ion-ion-structure factor. <i>Karakhtanov V.S., Redmer R., Reinholz H., Röpke G., IPCP RAS, U. Rostock</i>	33
4	Dense hydrogen	34
4.1	Thermodynamic properties of isentropically compressed hydrogen (deuterium) of megabar range <i>Gryaznov V.K., Iosilevskiy I.L., Fortov V.E., IPCP RAS, JIHT RAS</i>	34
4.3	Conductivity of multiple shock compressed hydrogen along 135 and 180 GPa isobars <i>Ternovoi V.Ya., Pyalling A.A., Nikolaev D.N., Kvitov S.V., IPCP RAS</i>	34

5	Laser and heavy-ion-produced plasmas	36
5.2	Ability of plasma to absorb laser radiation depending on the angle of its interaction <i>Khaydarov R., Beisinboeva H., Kholboev A., IAPh-Tashkent</i>	36
5.4	Simulations of Shock and Quasi-Isentropic Compression Experiments Driven by Intense Heavy Ion Beams <i>Grinenko A., Gericke D.O., Varentsov D., Vorberger J., GSI, Warwick</i>	37
5.5	Comparison of two theories during self focusing of laser beams in relativistic plasma. <i>Walia K., Singh A., NIT Jalandhar</i>	38
5.6	Potential of the Large Hadron Collider at CERN to Study High Energy Density Physics <i>Tahir N.A., Schmidt R., Shutov A., Lomonosov I.V., Piriz A.R., Hoffmann D.H.H., Fortov V.E., Deutsch C., CERN, GSI, JIHT RAS, IPCP RAS, LPGP, TU Darmstadt, UCLM</i>	38
5.8	Specific features of spallation processes in a Plexiglas (PMM) under high strain rate <i>Krasyuk I.K., Geraskin A.V., Khishchenko K.V., Pashinin P.P., Semenov A.Y., Vovchenko V.I., GPI, JIHT RAS</i>	39
5.9	Dense Xenon Nanoplasmas in Intense Laser Fields <i>Hilse P., Bornath T., Moll M., Schlanges M., U. Greifswald, U. Rostock</i>	40
5.11	Experimental investigation of femtosecond laser ablation spectral thresholds, condensed matter-dense plasma phase transition dynamics in ambient and vacuum conditions <i>Loktionov E.Y., Ovchinnikov A.V., Protasov Y.Y., Sitnikov D.S., BMSTU, JIHT RAS</i>	41
5.17	Non Linear propagation of intense laser beams through collisional plasmas <i>Walia K., Singh A.</i>	42
6	Dense astrophysical plasmas	43
6.4	Low-velocity ion stopping in binary ionic mixtures <i>Fromy P., Deutsch C., Tashev B.A., Baimbetov F.B., IETP KazNU, Paris Sud</i>	43
7	Phase transitions in plasmas and fluids	44

7.1	Fluctuation approach to the nonideal plasma equation of state calculation.	
	<i>Saitov I.M., Lankin A.V., Norman G.E., JIHT RAS</i>	44
7.3	Sound velocity measurements behind the shock wave in tin	
	<i>Zhernokletov M.V., RFNC-VNIIEF</i>	45
7.5	The Investigation of Phase Changes in Cerium and Titanium by PVDF-gauges	
	<i>Borisenok V.A., Zhernokletov M.V., Simakov V.G., Zocher M.A., Cherne F.J., LANL, RFNC-VNIIEF</i>	45

1 Statistical physics and mathematical modeling of strongly coupled Coulomb systems

1.1 Mathematical simulation of kinetic processes in the non-ideal nuclear-excited dust plasma of the noble gases

**Budnik A.P., *Deputatova L.V., Fortov V.E., Kosarev V.A.,
Rykov V.A., Vladimirov V.I.**

JIHT RAS, Moscow, Russia

**dlv@ihed.ras.ru*

The present report is devoted to the studying kinetic processes in the nuclear-excited plasma of the noble gases in which are injected the fine uranium (or its chemical compounds) particles.

More than 30 years passed since it was suggested to use such medium containing micro particles for converting of nuclear energy into optical radiation. Recently it has been shown, that application of the uranium nanoclusters or its chemical compounds for this purposes creates the new amplified laser radiation active medium excited by fission fragments of heavy nuclei. The main goal of this investigation is to determine possibilities of creation non-ideals dust plasma, containing nano- and micro-particles, and excited by fission fragments.

A new theoretical model for the mathematical simulation of the kinetic processes in dust plasma of helium gas was developed. System of equation for self-consistent description of the kinetic processes in the dust plasma of noble gas and for calculation properties for nuclear pumped media is derived. The self-consistent mathematical simulation of the kinetic process in the nuclear pump laser medium with the fine uranium particle admixture was performed at the first time.

A new algorithm for mathematical simulation kinetic processes in dust plasma of helium gas was developed. The main goal of the new model is including in consideration both, the multiply charged ions, as well as multiply charged fine particles. It was suggested that fine particles have spherical form with radii from 5 nm up to 0.2 μm . The plasma-chemical reactions with fine particles charged up to 40 electrons were considered.

It was shown that under typical conditions of the nuclear pumping the active laser medium may became non-ideal dust plasma.

Researches are spent at support of the Russian fund of basic researches (the project N 08 08 00456 and 07-08-13612).

1.3 Calculation of canonical properties and excited states by path integral numerical methods

*¹Vorontsov-Velyaminov P.N., ¹Voznesenskiy M.A., ¹Polyakov E.A.,
²Lyubartsev A.P.

¹SPbSU, Saint-Petersburg, Russia, ²SU, Stockholm, Sweden

*voron.wgroup@gmail.com

Path integral Monte Carlo method in the expanded ensemble [1] is used for calculation of the ratio of partition functions for different classes of permutations [2] treating the problem of several interacting identical particles (fermions) in an external field. Wang-Landau algorithm is used for adjustment of balancing factors. The complete partition function and average energy is then obtained at finite temperatures down to their low values. Calculations were performed for systems of two and three particles with Coulomb repulsion in 1D and 3D harmonic and 3D Coulomb external fields [3,4]. For systems consisting of greater number of particles we propose a new variant of our approach which implies calculation of the ratio of positive and negative contributions to the partition function.

Densities and energies of the sequence of excited states starting from the ground state for a system of non interacting quantum particles are calculated in turn, one by one, by means of considering systems with artificially excluded lowest energy levels and further obtaining of the "ground state" of each next system constructed in this way. These artificial systems are constructed with the aid of a recurrent sequence of propagators. It becomes possible to reproduce several tens of energy levels for the harmonic and other 1-dimensional potentials with a small expense of computer time. The main advantage of this numerical approach is that it is not constrained to the sign problem for Fermi particles. It can also be extended to 2- and 3-dimensional potentials [5,6].

[1] Lyubartsev A.P., Martsinovsky A.A., Shevkunov S.V., Vorontsov-Velyaminov P.N. J.Chem.Phys. **96(3)** (1992), 1776.

[2] Lyubartsev A.P., Vorontsov-Velyaminov P.N. Phys. Rev. A. **48** (1993), 4075.

[3] Wang F., Landau D.P. Phys. Rev. Lett. **86(10)** (2001), 2050.

- [4] Voznesenskiy M.A., Vorontsov-Velyaminov P.N., Lyubartsev A.P. Computational Methods and Programming **9** (2008), 170 (in russian).
- [5] Broukhno A.V., Vorontsov-Velyaminov P.N., Bohr H. Phys. Rev.E **72** (2005), 046703.
- [6] Polyakov E.A., Vorontsov-Velyaminov P.N. Computational Methods and Programming **8** (2007), 334 (in russian).

1.4 Investigation formation of charge and of energy spectra of multiply charged ions, generated under the action of laser radiation on the surface of two-element targets Tm_2O_3 , Yb_2O_3 and Eu_2O_3

***Khaydarov R., Berdierov G.**

IAPh-Tashkent, Tashkent, Uzbekistan

**rkhaydarov@nuuz.uzsci.net*

In continuation of our study of two-element laser-produced plasmas [1] we performed experiments on heavier elements targets (Tm_2O_3 , Yb_2O_3 , Eu_2O_3). The reason for the choice of these elements is that, although these differ considerably in mass, they have similar thermo physical parameters like conductivity, melting temperature, heat capacity, ionization potential etc. Experiments are carrier out in a laser-mass-spectrometer and we constructed energy spectra of ions on the base of obtained time-of-flight (mass-charge) spectra. Experimental results shows that oxygen ions with charge $Z=1, 2$ are located in a low energy part of the spectra and Tm, Yb and Eu ions are in larger energy part of the spectra. Energy spectra of Tm ions are shifted to larger energies as compared to energy spectra of Eu ions. We found that characteristics of energy spectra (the maximal energy E_{max} , width of the energy spectra) of light O^{1+} and O^{2+} ions strongly depend on the mass of the second component of the target: for a given intensity of the laser radiation the maximal width (i.e. the maximal energy) of energy spectra of single charged oxygen ions is obtained for the case of Yb_2O_3 and the minimal width is obtained for Tm_2O_3 . The maximal energy of O^{2+} ions does not depend on the mass of the heavy component of the target. However, a small dependence of energy distribution of O^{2+} ions on the nature of the target is found in a narrow energy range (60 – 120 eV), where recombination process is dominating. These dependencies vanish at small energy ranges (40 – 60 eV), where ionization process is dominating. Thus, the increase of the second component of the two-element plasma leads to the increased energy exchange between light (O)

and heavy (Tm, Yb, Eu) ions and to the expansion of the energy spectra of light ions to larger energies. The mechanisms of formation of energy spectra of ions in two-element laser-produced plasma and experimental outcomes in scientific and applied aspects are discussed.

[1] Khaydarov R.T. and al. International Journal of Plasma Science and Engineering **2008**, 180950.

1.7 Quantum Potential including Diffraction and Exchange Effects

^{*2}Dufty J.W., ²Dutta S., ¹Bonitz M., ¹Filinov A.V.

¹CAU, Kiel, Germany, ²U. Florida, Gainesville, USA

*dufty@phys.ufl.edu

An ideal Bose or Fermi gas interacting with an impurity is represented by a classical fluid with effective particle-particle and particle-impurity quantum potentials. The quantum potentials are evaluated at weak coupling, leading to generalizations of the Kelbg potentials to include both diffraction and degeneracy effects [1]. This potential is compared with previous effective pair potentials.

Furthermore, a phenomenological extension to strong coupling is proposed which is based on the “improved Kelbg potential” [2] which is applicable to strongly correlated quantum plasmas via incorporation of exact short range effects. The resulting quantum potential is tested by comparison with Path integral Monte Carlo results as a function of degeneracy.

[1] J. Dufty, S. Dutta, M. Bonitz, and A. Filinov, Int. J. Quant. Chem. (in press); arXiv:0903.2968v1.

[2] A. Filinov, V. Golubnychiy, M. Bonitz, W. Ebeling, and J. Dufty, Phys. Rev. E **70** (2004), 046411.

1.9 Semi-Classical Model of Strongly Correlated Coulomb Systems in Weak Magnetic Field

Ciftja O.

PVAMU, Prairie View, Texas 77446, USA

ogciftja@pvamu.edu

The integer and fractional quantum Hall effects are two remarkable macroscopic quantum phenomena occurring in two-dimensional strongly correlated electronic systems at high magnetic fields and low temperatures. Quantization of Hall resistivity indicates the onset of a novel electronic quantum Hall phase of matter that generally stabilizes in the very high magnetic field regime at partial filling of the lowest Landau level. Other interesting phases that differ from the quantum Hall phases take prominence in weaker magnetic fields when many more Landau levels are filled. These states manifest anisotropic magneto-transport properties and, under certain conditions, appear to mimic charge density waves and/or liquid crystalline phases. One way to understand such a behavior has been in terms of effective interaction potentials confined to the highest Landau level partially filled with electrons. In this work we show that, for weak magnetic fields, such a quantum treatment of these strongly correlated Coulomb systems resembles a semi-classical model of rotating electrons in which the time-averaged interaction potential can be expressed solely in terms of guiding center coordinates. We discuss how the features of this semi-classical effective potential may affect the stability of various strongly correlated electronic phases in the weak magnetic field regime.

1.11 Interfacial Properties of the Strongly Coupled Imidazolium Ionic Liquids: a Molecular Dynamics Study

*Kislenko S.A., Samoylov I.S., Amirov R.H.

JIHT RAS, Moscow, Russia

**kislenko@ihed.ras.ru*

Imidazolium ionic liquids are promising candidates for using in heterogeneous systems such as supercapacitors, fuel cells, solar cells, an operating efficiency of which is greatly influenced by the molecular structure of the electrode/electrolyte interface. However, the interfacial properties of such strongly coupled coulomb systems, composed of asymmetric bulky ions, are not well characterized.

This work reports the results from the molecular dynamics simulation of the ionic liquid [BMIM][PF₆] (with the nonideality parameter in the range of $\Gamma = e^2 n^{1/3} / (kT) \sim 60 \div 80$) on a graphite surface.

For the uncharged surface the temperature dependence (300 \div 400 K) of the interface structure and ions dynamics were investigated. It is shown that a near-graphite-surface ionic liquid has a layering structure, extending over ~ 2 nm from the surface [1]. In the vicinity of the wall self-diffusion

coefficients of ions correlate with the local ion density. From the free energy profiles it is revealed that ions absorption/desorption is a multibarrier activated process. The rate constants of cation and anion absorption/desorption was calculated.

The influence of the surface potential on the distribution of electrolyte ions and their orientation was studied. Increase in the electrode potential induces broadening of the angle distribution of adsorbed imidazolium rings and a shift of the most probable tilt angle towards bigger values.

In addition, the influence of the surface charge ($\pm\sigma$) on the volume charge density and electric potential profiles in the ionic liquid was determined. The differences in the cation and anion molecular structure result in the fact that potential profiles have an asymmetric form when the surface charges are equal in their magnitudes and opposite in sign.

A good agreement of the model predictions with experiments is obtained.

We would like to acknowledge the Joint Supercomputer Center of RAS for the computational resources placed at our disposal.

[1] Kislenco S.A., Samoylov I.S., Amirov R.H., Phys. Chem. Chem. Phys. **11** (2009), 5584.

1.13 Specific Features of Spallation Processes in Polymethylmetacrylate under High Strain Rate

*¹Krasyuk I.K., ¹Geraskin A.A., ³Khishchenko K.V., ¹Pashinin P.P.,
²Semenov A.Y., ¹Vovchenko V.I.

¹GPI, Moscow, Russia, ²IEP UB RAS, Ekaterinburg, Russia, ³JIHT RAS,
Moscow, Russia

*krasyuk99@rambler.ru

Direct laser interaction and laser-driven thin foils were used for investigation spallation phenomena in polymethylmetacrylate (PMMA) targets in case of high value of strain rates. In experiments the aluminium foils with thickness 8 and 15 μm were used as impactors. The laser-driven foils mass and velocity after laser ablation and acceleration were determined by the method of their deceleration in a gas atmosphere. On the basis of experimental data we measured the position of the spallation plane and the moment at which the spall layer arrived at an additional electrocontact sensor arranged beside of rear side of target. Then, the values of spall strength and strain rate were determined by the using numerical simulations with a hydrodynamic code

with a wide-range semi-empirical equation of state of PMMA. As a result of experiments, we found in the first time that in case of strain rate varying from $1.5 \cdot 10^6$ to $6 \cdot 10^6$ 1/s the ultimate spall strength of PMMA (10 kbar) was achieved.

1.14 Transition of Electromagnetic Wave Through a Warm Overdense Plasma

***²Rajaei L., ¹Mirabotalebi S.**

¹AU, Tehran, Iran, ²QOMU, Qom, Iran

*l-rajaei@Qom.ac.ir

It is studied a high transparency condition of an overcritical warm plasma layer due to the excitation of the electromagnetic surface modes. This procedure requires evanescent incident waves on the plasma layer which here is prepared by placing two dielectric layer on the both sides of the plasma film. Corresponding consequences for a cold plasma is also discussed and a comparison between cold and warm plasmas is also made.

1.15 Coulomb systems' modeling under consideration of finite instrumental resolution scales

Minkova N.R.

TSU, Tomsk, Russia

nminkova@mail.tomsknet.ru

Traditional description of plasma is based on one-particle kinetic equations for electrons and ions what implies that all coordinates of particle are considered as distinguishable. Long-range Coulomb interaction between particles is modeled by a mean field and collision integral.

Finite instrumental resolution scales restricts observer's ability to distinguish particles coordinates within these scales what results in plasma modeling based on distributions of *joint* probability that particles occupy a probing volume [1]. This *multiparticle* approach produces the description in terms of *fluctuations* of plasma parameters. The generated multiparticle models can be reduced under some assumptions to smaller dimensions but long-range interaction of particles does not allow us to linearize them to one-particle models in difference from the classical statistical theory.

Finite instrumental resolution scales' modeling is discussed in the paper (including Gibbs' paradox and a transition from a classical statistical integral to a quantum statistical sum) and demonstrated in application to solar plasma.

[1] Minkova N.R. *Contrib. Plasma Phys.* **49(1)** (2009), 90.

1.16 Ionization cross section for strongly coupled hydrogen plasma with arbitrary ionization degree

Baimbetov F.B., *Kudyshev Z.A.

IETP KazNU, Almaty, Kazakhstan

**z.kudyshev@mail.ru*

As it was shown in [1,2], it is very important to take into account the influence of plasma surrounding on the ionization process. The present work is aimed at the generalization of some previous results to the case of arbitrary ionization degree. The ionization cross section is calculated with help of pseudopotential model of plasma particles interaction, which takes into account correlation effects [3].

The electron impact ionization cross section is calculated from phase shifts of scattered and emitted electrons determined within the quantum mechanical approach in Born approximation [4, 5].

Comparison is made with the previous work, experimental data of [6] and suitable results represented in [7].

- [1] F.B. Baimbetov, Z.A. Kudyshev, *Journal of Physics: Conference Series* **112** (2008), 042085.
- [2] F.B. Baimbetov, Z.A. Kudyshev, *Journal of Physics: Mathematical and Theoretical Series*, (accepted) (2008).
- [3] F.B. Baimbetov, Yu.V. Arkhipov, A.E. Davletov, *Physics of Plasma* **12** (2005), 082701.
- [4] F. Calogero, *Variable phase approach to potential scattering*, Academic Press, New York, 1967 (translated into Russian in 1972).
- [5] N. Mott and H. Massy, *The theory of atomic collisions*, Oxford University Press (1949).
- [6] M.B. Shah, D.S. Elliot and H.B. Gilbody, *J. Phys B* **20** (1987), 3501.
- [7] Y.K. Kim and M.E. Rudd, *Phys. Rev. A* **50** (1994), 3954.

1.17 Modeling of Dielectrics Bombardment with Swift Heavy Ions

*Ivanov D.S., Osmani O., Rethfeld B.

TUKL, Kaiserslautern, Germany

**ivanov@rhrk.uni-kl.de*

The process of nanostructuring as a result of swift heavy ions penetrating a solid or its scattering on a surface has attracted a lot of scientific interest for the last decade. Especially, possible applications of the heavy ion bombardment technique have spawned in IT- and Bio- technologies. The processes of fast energy deposition into the solid and its further dissipation, however, are essentially perturbed with highly excited and nonequilibrium state of both lattice and electron systems. Meanwhile, the precision in treatment of such processes as thermalization of electrons, fast electron heat conduction, and the phase transformation of the overheated solid becomes crucial when considering the mechanism of nanostructures formation. Having several computational techniques to handle the mentioned processes it is nevertheless difficult to describe all of them within a scale of a single physical model.

Our work is aimed on elaboration of the atomistic-continuum computational approach to study the formation of nanohillocks in the experiments on swift heavy ion Xe^+ bombardment of SrTiO_3 [1]. The combined computational approach includes the description of fast ion energy deposition by Density Functional Theory [2], continuum description of the electron heat conduction and the electron-phonon energy transfer with Two Temperature Model [3], and nonequilibrium phase transformation at atomic level with Molecular Dynamics [4]. An advanced Ewald summation method is used to account for long range Coulomb interactions represented by ionic two body potential [5]. The resulted atomistic-continuum model is outlined and applied to study nonequilibrium phase transformations induced by a heavy projectile of high energy.

- [1] E. Akcoeltekın, S. Akcoeltekın, O. Osmani, A. Duvenbeck, H. Lebius, M. Schleberger, *New J. of Phys.* **10** (2008), 053007.
- [2] O. Osmani, A. Duvenbeck, E. Akcoeltekın, R. Meyer, H. Lebius and M. Schleberger, *J. Phys: Condens. Matter* **20** (2008), 315001.
- [3] S.I. Anisimov, B.L. Kapeliovich, and T.L. Perelman, *Zh. Eksp. Teor. Fiz.* **66** (1974), 776.

- [4] T. Katsumata, Y. Inaguma, M. Itoh, and K. Kawamura, *Solid State Ionics* **108** (1998), 175.
[5] A.Y. Toukmaij and J.A. Board Jr., *Comp. Phys. Comm.* **95** (1996), 73.

1.23 Formation of the globular defects in fluorite-like ionic crystals

¹Yakub L.N., ^{*2}Yakub E.S.

¹OSAR, Odessa, Ukraine, ²OSEU, Odessa, Ukraine

*yakub@oseu.edu.ua

Self-assembling processes of the defects clusters in hyper-stoichiometric and metastable stoichiometric crystals with fluorite structure was studied by molecular dynamics (MD) method. MD simulation program developed for ionic solids like UO_2 based on partially-ionic model [1] was applied in the study to the relative stability of different types of defects and evolution of the defects concentration in metastable UO_2 solid.

To destroy the less stable anionic sublattice, we applied a method of the thermal shock, i.e. short initial overheating period, which started at the temperature well above the melting temperature, and followed by series of the fast quenching/annealing periods (sudden or step by step temperature drops). To avoid melting of the cationic sublattice, thermal shock period was limited to a few picoseconds. During the whole MD simulation, we monitored the number and type of defects forming in the cell and computed their formation energies. The resulting structure of the relaxed solid was analysed using JMol visualization software. Along with formation of small (Willis) dimers of different types, we observed self-assembling of large regular globular structures.

Such structures in MD simulation can be observed only in a very large MD cells. In our simulation of stoichiometric UO_2 on desktop PC we used the fast method of computing of Coulomb forces proposed earlier [2] what gives us the possibility to use a cell containing 1200 ions ($20 \times 20 \times 20$ unit cells).

It was found that in hyperstoichiometric or thermally shocked stoichiometric solid under conditions when the thermal motion is restricted, the defects interaction leads mainly to the self-assembling of the very stable globular structures, containing 12 or 13 interstitial anions and eight lattice vacancies (cuboctahedral clusters). Such clusters have been found experimentally in hyper-stoichiometric fluorite crystals, but have never been observed at stoichiometric conditions yet.

- [1] E. Yakub, C. Ronchi and D. Staicu. J. Chem. Phys. **127** (2007), 094508.
[2] E. Yakub and C. Ronchi. J. Chem. Phys. **119** (2003), 11556.

2 Equilibrium properties and equation of state of dense plasmas

2.2 Phase shifts and the second virial coefficient for a partially ionized Hydrogen plasma

¹Ramazanov T.S., ^{*2}Omarbakiyeva Y.A., ²Röpke G.

¹IETP KazNU, Almaty, Kazakhstan, ²U. Rostock, Rostock, Germany
^{*}yultuz@physics.kz

The thermodynamic properties of Coulomb systems can be obtained from the virial expansions. The exact quantum mechanical expression for the second virial coefficient was given by Beth and Uhlenbeck [1]. They showed that the second virial coefficient can be expressed in terms of scattering phase shifts and bound state energies.

A partially ionized dense plasma is investigated, which consists of three components as electrons, ions and Hydrogen atoms. The second virial coefficients for the charged components $e-e$, $e-i$ and $i-i$ was already considered in Refs. [2, 3], but the coefficients for $e-H$ and $H-H$ pairs still present large interest.

The phase shifts for atom-atom scattering were calculated using the wave expansion method. Different pseudopotentials were considered to describe the interaction between atoms.

For the $e-H$ pairs, the second virial coefficient was calculated using experimental and theoretical values for the phase shifts in the singlett and triplett channel. A separable potential was constructed to reproduce these phase shifts. Within a generalized Beth-Uhlenbeck approach, density effects such as Pauli blocking have been incorporated. Thermodynamic and transport properties of partially ionized Hydrogen plasma are considered within our approach.

[1] Beth E, Uhlenbeck G E *Physica* **4** (1937), 915.

[2] Kraeft WD, Kremp D, Ebeling W, Roepke G *Quantum Statistics of Charged Particle Systems* (1986) (Berlin:Verlag).

[3] Kremp D, Kraeft WD, Schlages M *Contr.Plasma.Phys.* **33** (1993), 567.

2.3 Electrical resistivity in warm dense plasmas beyond the average-atom model

***Pain J.C., Dejonghe G.**

CEA, Bruyères-le-Château, France

**jean-christophe.pain@cea.fr*

The exploration of atomic properties of strongly coupled partially degenerate plasmas, also referred to as warm dense matter, is important in astrophysics, since this thermodynamic regime is encountered for instance in Jovian planets' interior. One of the most important issues is the need for accurate equations of state and transport coefficients. The Ziman formula has been widely used for the computation of the static (DC) electrical resistivity. Usually, the calculations are based on the continuum wave-functions computed in the temperature- and density-dependent self-consistent potential of a fictive atom, representing the average ionization state of the plasma (average-atom model). We present calculations of the electrical resistivity of a plasma based on the superconfiguration (SC) formalism. A SC is made of groups of orbitals (namely super-orbitals) with integer electron populations. In this modeling, the contributions of all the electronic configurations are taken into account. It is possible to obtain all the situations between the two limiting cases: detailed configurations (a super-orbital is a single orbital) and detailed ions (all orbitals are gathered in the same super-orbital). The ingredients necessary for the calculation are computed in a self-consistent manner for each SC, using a density-functional description of the electrons. Electron exchange correlation is handled in the local-density approximation. The momentum transfer cross-sections are calculated by using the phase shifts of the continuum electron wave-functions computed, in the potential of each SC, by the Schrödinger equation with relativistic corrections (Pauli approximation). Comparisons with experimental data will also be presented.

2.4 Modeling of Thermodynamic Properties of Dense Multicharged-Ion Plasmas Based on the Chemical-Picture Approach

***Shadrin A.A., Loboda P.A., Popova V.V.**

RFNC-VNIITF, Snezhinsk, Russia

**a.a.shadrin@mail.ru*

Consistent modeling of thermodynamic properties of dense plasmas in the warm-dense-matter domain is still one of the challenging problems to be addressed. Using the chemical-picture representation of plasmas as a mixture of various ions and free electrons [1, 2], a consistent description of thermodynamics of dense multicharged-ion plasmas is being developed that involves: effects of Coulomb non-ideality and degeneracy of plasma electrons; contribution of possible bound ion states (on the base of the superconfiguration approach [3]) that may exist under an appropriate truncation of ion energy spectra due to plasma effects; hard-sphere-model representation of the finite-volume effects of plasma ions [3] with the model parameters (effective ion sizes) corresponding to superconfigurations yielding the greatest contribution to partition functions. We present the calculated data for average ionization, pressure, specific internal energy, and specific heat of aluminum and iron plasmas at temperatures 30 eV - 3 keV and densities $10^{-3} - 10^{-5}$ of their normal material densities. Calculated shock Hugoniot and thermodynamic functions are compared with other theoretical and experimental data.

The work has been supported by the International Science and Technology Center under the project Nr. 3755.

- [1] D.G. Hummer and D. Mihalas. *Astrophys. J.*, **331** (1988), 794
- [2] V.K. Gryaznov, I.L. Iosilevsky, V.E. Fortov. *Thermodynamic properties of shock-compressed plasmas represented with the chemical-picture model*, in: *Shock waves and Extreme States of Matter*, V. E. Fortov et al. eds., Nauka, Moscow, 2000, pp. 342-387 [in Russian]
- [3] J. Oreg, A. Bar-Shalom, M. Klapisch, *Phys. Rev. E.*, **55** (1997), 5874.

2.8 Dielectric catastrophe and insulator-metal transition in AlH_3 .

*²**Khrapak A.G.**, ¹**Molodets A.M.**, ¹**Shakhrya D.V.**, ²**Fortov V.E.**

¹*IPCP RAS, Chernogolovka, Russia*, ²*JiHT RAS, Moscow, Russia*

* *khrapak@mail.ru*

A study of properties of alane (AlH_3) under multi shock compression has been carried out. The increase in specific conductivity of alane at shock compression up to pressure 100 GPa has been measured. The compression loads the alane sample by multi shock manner up to the pressure 80 – 90 GPa, heats it to the temperature about 1500 – 2000 K and lasts 1 microsecond. The conductivity of shocked alane increases in the range up to 60 – 75 GPa and is about

$30 \text{ (}\Omega\text{m cm)}^{-1}$. In this region the semiconductor regime is true for shocked alane. The conductivity of alane achieves approximately $500 \text{ (}\Omega\text{m cm)}^{-1}$ at 80 – 90 GPa. In this region conductivity is interpreted in frames of the conception of the “dielectric catastrophe”, using Herzfeld-Goldhammer criterion. According to this criterion, the dielectric-conductor transition takes place when permittivity of a matter begins to rise sharply and amounts to values exceeded unity significantly. In the case of AlH_3 it is necessary to take into account that outer electrons of the Al are transferred to the H atoms and the permittivity is determined by the polarizability of ions Al^{3+} (can be neglected) and H^- . The exchange interaction between electrons of the neighboring ions H^- results in significant decrease of the region occupied by each electron and in decrease of the ion polarizability. Our estimation of the polarizability of the alane molecule in condensed state gave a value equal to 9.6 a.u. With such polarizability the “dielectric catastrophe” and, consequently, dielectric-conductor transition have to begin at $n = 5.6 \cdot 10^{22} \text{ cm}^{-3}$ or $\rho = 2.8 \text{ g cm}^{-3}$, what is in agreement with our results and with experiments of Goncharenko *et al.* (2008). Proposed model can be used for estimations of the transition density to the conductive state for other metal hydrides such as MgH_2 , NaH, and LiH. Possible mechanism of the alane conductivity is following. At normal conditions valence electrons of aluminum are trapped by hydrogen atoms forming negative ions H^- . The resulting electron energy band is fully occupied and condensed alane is a good insulator. By increasing the temperature a part of the electrons turns to aluminum, neutral atoms of hydrogen appear in the system and migration of electrons from H^- to H becomes possible. Such mechanism of the electron transfer can explain the semiconductor character of the alane conductivity observed in experiment. By increasing the density the permittivity also increases. This results in the decrease in electron binding energy in ion H^- and, consequently, in the decrease in band gap. At high enough density the permittivity becomes infinite, the band gap disappears, and the conductivity gains the metallic character.

2.10 Use of Pulsed Radiography for Investigation of Equation of States of Substances at Megabar Pressures

Egorov N.I., Boriskov G.V., *Bykov A.I., Kuropatkin Yu.P.,
Luk'yanov N.B., Mironenko V.D., Pavlov V.N.

RFNC-VNIIEF, Sarov, Russia

*bykov@ntc.vniief.ru

A method of substances densities measurement that are isentropically compressed up to megabar pressures is described in the paper. Measurement results of densities of condensed hydrogen and aluminum isotopes are presented. These results, afterwards, are used for hydrogen isotopes equations of state construction. Experimental x-ray images of the facilities with the hydrogen isotopes, compressed up to several megabars are presented in the paper.

2.11 Multiphase equation of state for iron at high pressures and temperatures

Khishchenko K.V.

*JIHT RAS, Moscow, Russia
konst@ihed.ras.ru*

An equation of state of different materials over a wide range of parameters is necessary for numerical simulations of physical processes in plasmas at high energy densities. Reliability of the calculation results is determined mainly by adequacy of description of thermodynamic properties of a medium. In the present work, a new semiempirical model of thermodynamic potential free energy with taking into account polymorphic phase transitions, melting and evaporation is presented for metals. On the basis of this model, multiphase equation-of-state calculations are carried out for iron at high pressures and temperatures. Obtained results are in a good agreement with available experimental data on shock compression as well as adiabatic and isobaric expansion.

2.14 Semiempirical equations of state for metals based on Thomas–Fermi model

***Shemyakin O.P., Khishchenko K.V.**

*JIHT RAS, Moscow, Russia
shemyakin@ihed.ras.ru

For analyzing the physical processes at high energy densities, an adequate description of the thermodynamic properties of matter over a broad region of states including both the condensed phase under normal conditions and plasma at high pressures and temperatures is required. In the present work, a semiempirical equation-of-state model, which is based on Thomas–Fermi

theory [1], is proposed. According to this model, the Helmholtz free energy for matter is considered as a sum of three components, $F(V, T) = F_c(V) + F_a(V, T) + F_e(V, T)$, describing the elastic part of interaction at $T = 0$ K (F_c) and the thermal contributions of heavy particles (atoms, ions, nuclei) and electrons (F_a and F_e , respectively). The first and second components are given by interpolation formulae, the third is calculated within the framework of the Thomas–Fermi model [1]. Wide-range equations of state are developed for aluminum and copper. A critical analysis of calculated results in comparison with available experimental data for these metals at high pressures and temperatures is made.

[1] R. Feynman, N. Metropolis, E. Teller. *Phys. Rev.* **75** (1949), 1561.

2.15 Thermodynamic Properties of Gaseous Plasmas in the Zero-Temperature Limit

Iosilevskiy I.L.

JIHT RAS, Moscow, Russia

ilios@orc.ru

Limiting structure of thermodynamic functions of gaseous plasmas is under consideration in the limit of extremely low temperature and density ($T \rightarrow 0$; $n \rightarrow 0$). Remarkable tendency, which was claimed previously [1, 2], is carried to extreme. The discussed limit is carried out at fixed value for chemical potential of electrons or atoms or molecules *etc.* In this limit both equations of state (EOS) thermal and caloric one, obtain almost identical stepped structure (“ionization stairs” [2]). The same stepped structure appears in the zerotemperature limit in any molecular gases, for example hydrogen [3]. For rigorous theoretical proof of existing the limit, which is under discussion (Saha-limit) in the case of hydrogen see [4, 5] and references therein. In this zero-temperature limit all thermodynamic differential parameters (heat capacity, compressibility, etc.) obtain their remarkable σ -like structures (“thermodynamic spectrum” [2, 6]). Both kinds of such “spectrum” became apparent: i.e. “emission-like spectrum” for heat capacity and “absorption-like spectrum” for the isentropic exponent [3]. This limiting structure appears within a fixed negative range of μ_{el} (“intrinsic energy scale”) [2]. It is bounded below by value of major ionization potential. Binding energies of all possible bound complexes (atomic, molecular, ionic and clustered) in its ground state are the

only quantities that manifest itself as location and value of every step. The value depending on the heat of condensation at $T = 0$ supplement this collection. All the “lines” of the “thermodynamic spectrum” are centralized just at the elements of this “intrinsic energy scale”. The limiting EOS stepped structure (ionization stairs) of gaseous zero-Kelvin isotherm is generic prototype of well-known “shell oscillations” in EOS of gaseous plasmas at low, but finite temperatures and non-idealities [7]. The gaseous branch of discussed zero-Kelvin isotherm could be naturally conjugated with associated condensed branch. This combination creates complete and totally meaningful non-standard “cold curve” for any substance $\{U_0(\mu)$ instead of $U_0(\rho)\}$ [3]. All present statements about remarkable limiting structure of thermodynamic functions in zero-temperature limit for single substances are valid also in application to the chemical compounds [6].

- [1] Iosilevski I. High Temperature **19** (1981), 494.
- [2] Iosilevskiy I. Int. Conference “Physics of Non-Ideal Plasmas”, 2000.
- [3] Iosilevskiy I. Encyclopedia of low-temperature plasma physics, III-1, FIZMATLIT: Moscow, 2004, 349-428 (in Russian)
- [4] Brydges C. and Martin P. J. Stat. Phys. **96**(1999), 1163.
- [5] Alastuey A. and Ballenegger V. J. Phys. A: **42** (2009), 214031.
- [6] Iosilevskiy I., Krasnikov Yu., Son E., Fortov V. Thermodynamics and Transport in Non-Ideal Plasmas, MIPT Publishing: Moscow, 2000, 120-138 (in Russian); FIZMATLIT: Moscow, 2009, (in press).
- [7] Iosilevski I. and Gryaznov V. High Temperature **19** (1981), 799.

3 Kinetics, transport and optical properties of dense Coulomb systems

3.2 Magnetotransport properties of dense plasmas

*²Reinholz H., ³Adams J., ²Röpke G., ²Redmer R., ¹Shilkin N.S.,
¹Mintsev V.B., ¹Gryaznov V.K.

¹IPCP RAS, Chernogolovka, Russia, ²U. Rostock, Rostock, Germany, ³UWA,
WA6009 Crawley, Australia

**heidi.reinholz@uni-rostock.de*

The Hall coefficient is an important measure of the transport properties of a material in a magnetic field. We investigate whether the relationship of the Hall coefficient to the density of free charge carriers could provide a tool in plasma diagnostics [1]. Correlation effects in dense plasmas require a quantum statistical theory. Linear response theory, as developed within the Zubarev formalism, is a quantum statistical approach for describing systems out of but close to equilibrium, which has been successfully applied to a wide variety of plasmas in an external electric field and/or containing a temperature gradient. We present here an extension of linear response theory to include the effects of an external magnetic field [2]. All relevant transport properties are discussed, in particular the Hall effect and the influence of a magnetic field on the dc electrical conductivity [3]. New low-density limits including electron-electron scattering are presented. Additionally, we compare results from linear response theory with recent experiments in shock wave produced Ar and Xe plasmas [4]. The electrical conductivity and the Hall coefficient have been measured for free electron densities between 10^{14} and 10^{20} cm⁻³ and temperatures in the range 6000 K to 18000 K in a 5 Tesla field.

[1] J.R. Adams, H. Reinholz, R. Redmer, N.S. Shilkin, V.B. Mintsev, V.K. Gryaznov, *Contrib. Plasma Phys.* **47** (2007), 331.

[2] J.R. Adams, H. Reinholz, R. Redmer, M. French, *J. Phys. A* **39** (2006), 4723.

[3] J.R. Adams, H. Reinholz, R. Redmer, *subm. to PRE.*

[4] N.S. Shilkin et al., *Zh. Eksp. Teor. Fiz.* **124** (2003), 1030.

3.4 The calculations of transport coefficients of noble gases under high pressures

Apfelbaum E.M.

*JIHT RAS, Moscow, Russia
apfel.e@mail.ru*

The conductivity, thermal conductivity and thermopower of noble gases have been investigated during last several dozens years (see [1] for references). One of interesting process observed in experiments is the increase of the values of the transport coefficients with respect to their ordinary values under high pressures. This effect is analogous to the phenomena observed in metals in the vicinity of the critical point, which is known as dielectric–metal transition. This transition occurs because of the pressure ionization in both cases. It gives rise to a steep increase in the free electron density, which in turn results in a large increase in the electrical conductivity and other coefficients.

In spite of many theoretical works describing the behaviour of transport coefficients of noble gases there are still open questions. One of them concerns the change ionization degree during compression. Different ionization mechanisms are possible which can give rise to contradictions. For example, recently new experimental data have been obtained [2,3] by means of shock compression. To describe the results of the measurements there was used two numerical codes, which were created on the basis of the generalized chemical models. But calculated and measured conductivity for the experiments in hand can differ in two times [3].

In present report we try to apply different theories and models to the calculation of transport coefficients of noble gases (argon, xenon, krypton) under wide variation of densities and temperatures. The results of calculation were compared with available experiments and calculations of other authors.

[1] Q.F. Chen, L.C. Cai, Y.J. Gu, Y. Gy, Phys. Rev. E. **79** (2009), 016409.

[2] N.S. Shilkin et. al., Sov. Phys. JETP. **97** (2003), 922.

[3] J.R. Adams, H. Reinholz, R. Redmer, V.B. Mintsev, N.S. Shilkin, V.K. Gryaznov, Phys. Rev. E. **76** (2007), 036405.

3.6 On the replacement of collisional recombination mechanism in nonideal plasma.

Lankin A.V.

*MIPT, Dolgoprudny, Russia
lankin@ihed.ras.ru*

Dependence of collisional recombination mechanism on plasma parameters is considered. Whereas the coefficient C is a constant value in the formula for the collisional recombination rate in ideal plasma $K_e = CZ^3 e^{10} m^{-1/2} n_e^2 n_i T^{-9/2}$, the dependence of C on the nonideality parameter Γ and ion charge Z should be introduced for nonideal plasma. The boundary value of Γ depends on Z . The coefficient C decreases exponentially with the further increase of Γ for all Z . The following approximate expression is suggested $K_e = K_0 \Gamma^{9/2} \exp(-a\Gamma) \exp(-bZ\Gamma)$, where K_0 , a and b are constant values which are found by molecular dynamics simulation.

The change of Γ -dependence of C from the constant to exponentially decreasing function points to the change of recombination mechanism. Analysis of the bound electron-ion pair distributions over binding energies reveals the fact that Fokker-Planck diffusion is blocked for large Γ , isolated strong collisions becoming the predominant recombination mechanism. It is due to the extension of the energy interval of the many-particle fluctuations adjoining the ionization limit with the increase of Γ . The change of the mechanism takes place when the interval value exceeds the thermal energy.

3.8 Pressure Broadening of Spectral Lines in Dense Lithium Plasmas

***Lorenzen S., Wierling A., Reinholz H., Röpke G.**

*U. Rostock, Rostock, Germany
sonja.lorenzen@uni-rostock.de

Pressure broadening of Lyman-lines of hydrogen-like lithium (Li^{2+}) is studied using a quantum statistical approach to the line shape in dense plasmas, for details see [1]. We report line widths (FWHM) and shifts for Lyman- α , $-\beta$, and $-\gamma$ in a wide range of densities ($n_e = 10^{24} - 10^{28} \text{ m}^{-3}$) at temperatures relevant for laser-produced lithium plasmas ($T = 10^5 \text{ K}$). We discuss the effect of different ionic microfield distributions and estimate the influence of

ion dynamics. Special care is taken to account for strong collisions by using a microscopic treatment of the three-body T-matrix.

The results are applied to measured spectra of lithium irradiated by a nanosecond laser pulse of moderate intensities ($I \approx 10^{11} - 10^{13} \text{ W/cm}^2$), see [2]. By matching synthetic spectra to the experimental ones, density and temperature conditions are inferred assuming the model of a one-dimensional uniform plasma slab. Self-absorption is accounted for and found to be important for Lyman- α . In this way, experimental spectra are overall reproduced. To describe remaining deviations in the line wings, it is essential to use a multilayer model adapted to density and temperature profiles from hydrodynamic expansion codes.

Alternatively, we need time and space resolved spectra to compare theory and experiments, which are available for He-like lithium (Li^+), see [3]. Therefore, we also calculate the line profile of the $\text{Li}^+ 1s2p \rightarrow 1s2s$ transition at 548 nm, using our quantum statistical approach. Implications for the conversion efficiency are drawn.

- [1] S. Lorenzen et al., *Contrib. Plasma Phys.* **48** (2008), 657.
- [2] G. Schriever et al., *Applied Optics* **37** (1998), 1243; *J. Appl. Phys.* **83** (1998), 4566.
- [3] D. Doria et al., *Meas. Sci. Technol.* **17** (2006), 670.

3.9 Radiation Hydrodynamics of Laser-induced Plasmas using Dynamic Collision Frequencies

***Sperling P., Wierling A., Röpke G., Winkel M.**

U. Rostock, Rostock, Germany

**philipp.sperling@uni-rostock.de*

Radiation Hydrodynamics of laser-induced plasmas is usually treated by well-established hydrodynamic codes such as MEDUSA or MULTI. These codes require transport coefficients, e.g. absorption coefficients or thermal conductivity, as inputs. Typically, Spitzer-Härm-like expressions are used. However, for high densities these expressions can not be applied and have to be replaced by more advanced expressions. In particular, quantum effects and dynamical screening have to be accounted for in a systematic manner, see Reinholz et al. *PRE* **62**, 5648 (2000). Here, we present results of a hydrodynamical calculation including these advanced collision frequencies. We also compare to earlier

calculations with Spitzer–Härm–like expressions. In particular, the radiation hydrodynamics for laser-induced Lithium plasmas is studied. Conditions for optimal conversion efficiency are derived.

3.11 Quantum kinetic approach to time-resolved photoionization of multi-electron atoms

Bauch S., Hochstuhl D., Balzer K., *Bonitz M.

CAU, Kiel, Germany

**bonitz@physik.uni-kiel.de*

Recent progress in experiments [1], now often called ‘attophysics’, allows for time-resolved investigation of electronic processes in atoms and, ultimately also atoms in plasmas. The most prominent examples are the time-resolved measurements of Auger decay [2] and the dynamics of shake-up state population during strong field ionization of atoms [3]. These new fields of ultra-short time physics (‘attosecond chronoscopy’) require a time-resolved theory of ionization of multi-electron atoms by ultra-short XUV/UV pulses in combination with strong IR fields in pump-probe setups. On the way towards understanding and modeling these phenomena, we present first results of a quantum kinetic theory of ionization of simple few-electron model systems [4]. Approximate many-body approaches, in particular time-dependent Hartree-Fock and Multi-configurational-Hartree-Fock are compared to full solutions of the few-particle time-dependent Schrödinger equation. We further apply the technique of non-equilibrium Greens functions in second Born approximation to systematically account for electronic correlations and their attosecond dynamics in atoms subject to strong electromagnetic radiation.

[1] F. Krausz and M. Ivanov, *Rev. Mod. Phys.* **81** (2009), 163.

[2] M. Drescher et al., *Nature* **419** (2002), 803.

[3] M. Uiberacker et al., *Nature* **446** (2007), 627.

[4] D. Hochstuhl, K. Balzer, S. Bauch, and M. Bonitz, *Physica E* (accepted)

3.13 Atomic Database Spectr-W³ for Plasma Spectroscopy and Other Applications. Current Status and Perspectives

^{*3}Loboda P.A., ³Gagarin S.V., ³Kozlov A.I., ³Morozov S.V.,
³Popova V.V., ³Vanina I.A., ²Faenov A.Ya., ²Magunov A.I.,
²Pikuz T.A., ²Skobelev I.Yu., ¹Urnov A.M., ¹Vainshtein L.A.

¹FIAN, Moscow, Russia, ²JIHT RAS, Moscow, Russia, ³RFNC-VNIITF,
Snezhinsk, Russia

**p-a.loboda@mail.ru*

The Spectr-W³ information-reference system was developed in 2001–2003 and realized as an online Web resource based on the factual atomic database Spectr-W³ (<http://spectr-w3.snz.ru>). The information accumulated in the Spectr-W³ atomic database contains about 450,000 records and includes the experimental and theoretical data on ionization potentials, energy levels, wavelengths, radiation transition probabilities, and oscillator strengths, and the parameters of analytical approximations of electron-collisional cross-sections and rates for atoms and ions. Those data were extracted from publications in physical journals, proceedings of the related conferences, special-purpose publications on atomic data, provided directly by authors and obtained in previous years by the Spectr-W³ project participants. The information is supplied with references to the original sources and comments, elucidating the details of experimental measurements or calculations. To date, the Spectr-W³ atomic database is still the largest factual database in the world, containing the information on spectral properties of multicharged ions. In 2007 this collaborative effort was followed by a new project aimed at the creation of a qualitatively updated version of the Spectr-W³ atomic-data information-reference resource on the Web to provide free access to an essentially extended Spectr-W³ atomic database. Project activities are also targeted at the creation of facilities for direct submission of new author's atomic data for the follow-on dissemination through the Spectr-W³ resource and downloading the selected data in HTML or XML representation. Updated version of Spectr-W³ is also supplemented with its fully functional local analog (Spectr-CD) generated for the off-line use and available for downloading from the project website. The results of the project are intended for public and non-profit use. Current status of the project work will be outlined and illustrative results will be presented. The work has been supported in part by the International Science and Technology Center (ISTC) under the project Nr. 3504.

3.15 The modeling of the continuous absorption spectra of the dense hydrogen plasma on the base of the cut-off Coulomb potential

*Sakan N.M., Mihajlov A.A., Ignjatovic Lj.M., Sreckovic V.A.

IoP, Zemun-Beograd, Serbia

**nsakan@phy.bg.ac.yu*

The possibilities of the modeling of the continuous absorption spectra of the dense non-ideal plasma by means of the some cut-off Coulomb potentials are examined in this work on the dense hydrogen plasma example. The main aim was the development of the semi-empirical method suitable for the calculations of the spectral absorption coefficients characterizing the processes of the excited hydrogen atom photo-ionization and the electron ion inverse "bremsstrahlung". The corresponded method, presented in this work, was developed on the base of the data obtained in several experiments. The method is tested in the ranges of the electron densities and temperatures $1 \cdot 10^{18} \text{ cm}^{-3} \leq N_e \leq 1.5 \cdot 10^{19} \text{ cm}^{-3}$ and $10000 \text{ K} \leq T \leq 25000 \text{ K}$. The obtained results can be already used for the interpretation of the experimental results in wide area of the electron densities and temperatures, and they could clearly determine the direction of the further development of the model methods based on cut-off Coulomb potentials.

3.17 Interparticle interactions effect on behavior of caloric equation of state for plasma of dense metals vapor

*Shumikhin A.S., Khomkin A.L.

JIHT RAS, Moscow, Russia

**shum_ac@mail.ru*

State of the metals changed from the solid to gaseous state at Joule heat, there is occurs metal-nonmetal transition. Many experimental and theoretical papers are devoted to investigation of features of this transition. Pressure, internal energy and conductivity are experimentally measured for rapid heated metal wires and foils. We suggest the 7 components chemical model of dense metals vapor plasma consisting of electrons, atoms, single, double and triple ionized atoms, molecules and molecular ions. The model is used for calculation of caloric and thermal equations of state (EOS) and plasma composition. All

kinds of antiparticles interactions (charged-charged, charged-neutral, neutral-neutral) were considered. To take into account free charges interaction the Debye theory in grand canonical ensemble (BD) and nearest neighbor approximation (NNA) were used. Ion-atom interactions are considered in different approximation: second virial coefficient, virial coefficient with Hill correction, Likalter approximation. Electron-atom interaction was taken into account in scattering length approximation. Wigner approximation is used for estimation of scattering length using electron affinity. Pressure dependence on internal energy for isochors of various metals (aluminum, copper, titanium, gold) were calculated. The plasma resistivity in depend on internal energy was calculated using Frost's interpolation formula. The satisfactory agreement with experimental data is received.

3.19 Transport coefficients in dense plasmas including ion-ion-structure factor.

***¹Karakhtanov V.S., ²Redmer R., ²Reinholz H., ²Röpke G.**

¹*IPCP RAS, Chernogolovka, Russia, ²U. Rostock, Rostock, Germany*

**valera@chgnet.ru*

Within linear response theory, a general approach to the thermoelectric transport coefficients has been given. Different approximations for the collision integral are considered. Particular attention is drawn to dynamical screening and the ion-ion structure factor. Results are given for electrical conductivity and thermopower in comparison to earlier approaches as well as experiments.

4 Dense hydrogen

4.1 Thermodynamic properties of isentropically compressed hydrogen (deuterium) of megabar range

¹Gryaznov V.K., ^{*2}Iosilevskiy I.L., ²Fortov V.E.

¹*IPCP RAS, Chernogolovka, Russia*, ²*JIHT RAS, Moscow, Russia*
** ilios@orc.ru*

The data for three experiments on quasi-isentropic compression of dense hydrogen (deuterium) at megabar pressure range are under discussion and comparison with theoretical predictions. The main statement is claimed and supported that the results on relatively high-temperature compression [1, 2] and new results on relatively low-temperature compression [3], see also this conference) do not contradict nor confirm each other. Hypothetical theoretical explanations of density discontinuity, which were measured at high-temperature isentropic compression, are discussed.

[1] Grigor'ev et al. *Sov. JETF Lett.* **16** (1972).

[2] Fortov et al. *PRL* **99** (2007).

[3] Boriskov et al. *J.Phys.* **121** (2008).

4.3 Conductivity of multiple shock compressed hydrogen along 135 and 180 GPa isobars

^{*}Ternovoi V.Ya., Pyalling A.A., Nikolaev D.N., Kvitov S.V.

IPCP RAS, Chernogolovka, Russia
** ternovoi@icp.ac.ru*

The results of temperature and conductivity measurements of hydrogen, multiple shock compressed to the pressures 135 and 180 GPa are presented. Explosively driven steel plate with velocity up to 8 km/s was used for shock wave generation. Hydrogen with different initial pressures and temperatures was multiple shock compressed between steel bottom and sapphire window. Brightness temperature of hydrogen was measured by fast optical pyrometer. Electrical resistance of shocked hydrogen was measured simultaneously with optical pyrometer records.

The conductivity of hydrogen decreased from 424 $1/\Omega/cm$ at 2700 K down to 20 $\Omega^{-1}cm^{-1}$ at 6000 K along 135 GPa isobar. The conductivity of hydrogen decreased from 800 $\Omega^{-1}cm^{-1}$ at 5000 K down to 100 $\Omega^{-1}cm^{-1}$ at 6700 K along 180 GPa isobar. Experimental results are compared with different theoretical predictions.

Work was supported by the Program of Presidium of RAS P-09.

5 Laser and heavy-ion-produced plasmas

5.2 Ability of plasma to absorb laser radiation depending on the angle of its interaction

*Khaydarov R., Beisinboeva H., Kholboev A.

IAPh-Tashkent, Tashkent, Uzbekistan

**rkhaydarov@nuuz.uzsci.net*

We have conducted experiments in time-of-flight mass-spectrometer connected with electrostatic analyzer to determine the effect of absorbed energy to the charge and energy state of plasma as well as emission of ions. Investigations are conducted in two regimes. In the first case laser radiation with intensity $q = 10^{11}$ W/cm² interacted at the angles $\Theta \sim 20^\circ - 70^\circ$ with the targets made of Al, Fe and W and located perpendicular to the axis of the mass-spectrometer. In the second case the same laser interacts at the case angle with the plasma generated previously by the second laser with the same parameters as the first one.

It was found experimentally that, in both cases the laser radiation is more absorbed at small angles $\Theta \leq 23^\circ$. At the same time the charge and energy spectra of ions, as well as their emission increases more effectively in the second case. In both cases with increasing Θ from 20° to 70° the intensity of single charged ions increases while the intensity of highly charged ions decreases.

The analysis of energy spectra of ions in both regimes shows that with increasing Θ the shape of energy spectra for ions with charge $Z \geq 1$ practically does not change, although the maximum of the distribution shifts to lower energies. We also found that the maximum of the energy spectra depends not only on q but also on the mass of the target element A: at small interaction angles larger A leads to larger maximal energy, while for small Θ this dependence is not observed.

We also found that the effect of increased charge and energy state of plasma in the second case can be increased by delaying the laser radiation with $q = 10^{11}$ W/cm² relative to the laser with $q = 10^8$ W/cm², i.e. to form optimal condition for the consecutive heating of the plasma.

Considerable increase of ions charge in laser-produced plasma, formed in the second regime at small angles can be explained by the resonant absorption of laser radiation on the boundary of gradient of plasma density.

5.4 Simulations of Shock and Quasi-Isentropic Compression Experiments Driven by Intense Heavy Ion Beams

^{*2}Grinenko A., ²Gericke D.O., ¹Varentsov D., ²Vorberger J.

¹GSI, Darmstadt, Germany, ²Warwick, Coventry, United Kingdom

*A.Greenenko@Warwick.ac.uk

In this contribution, the capabilities of the new heavy-ion beam facilities at the Gesellschaft für Schwerionenforschung Germany, Darmstadt to drive laboratory astrophysics (LAPLAS) [1] and ramp wave loading experiments [2] are investigated.

A wide range hydrogen equation of state encompassing solids to high-temperature plasmas was constructed employing experimental data and first principles simulations. These EOS data were then used in our hydrodynamic simulation of LAPLAS targets. In the simulations, the transition of hydrogen from the frozen state at 14 K up to maximum of the melting line and beyond was considered. The results of the hydro-simulations indicate that, using the capabilities of the FAIR, it will be possible to access the regions of solid and fluid molecular hydrogen around the maximum of the melting line as well as the metallic fluid region. By careful tuning of beam parameters it should be possible to determine the hydrogen melting line in the high-pressure region.

Furthermore, a new design for heavy-ion beam driven ramp wave loading is suggested and analyzed. The proposed setup utilizes long stopping ranges and the variable focal spot geometry of the high-energy uranium beams, to produce a planar ramp loading of various samples. In such experiments, the predicted high pressures amplitudes (< 10 Mbar) and short timescales of the compression (< 10 ns) will allow testing the time-dependent material deformation phenomena at unprecedented extreme conditions.

[1] A. Grinenko et al., Phys. Rev. Lett., **101**, 194801 (2008).

[2] A. Grinenko et al., submitted to Phys. Rev. Lett.

5.5 Comparison of two theories during self focusing of laser beams in relativistic plasma.

*Walia K., Singh A.

NIT Jalandhar, Jalandhar, India

**keshavpaulwalia@gmail.com*

In the present paper, Self focusing of laser beams in relativistic plasmas is studied by moment theory approach. Equilibrium beam radius of self trapped laser beams is also derived. Results are compared with paraxial ray approximation. It is observed from the analysis that moment theory predicts almost flatter dependence of equilibrium beam radius on intensity than does paraxial ray approximation as intensity of beam increases. This is found to be true on account of saturating nature of relativistic non-linearity. So, the agreement between two theories worsens as the power of beam increases.

5.6 Potential of the Large Hadron Collider at CERN to Study High Energy Density Physics

*2Tahir N.A., ¹Schmidt R., ⁴Shutov A., ⁴Lomonosov I.V., ⁷Piriz A.R.,
⁶Hoffmann D.H.H., ³Fortov V.E., ⁵Deutsch C.

¹CERN, Geneva, Switzerland, ²GSI, Darmstadt, Germany, ³JIHT RAS,
Moscow, Russia, ⁴IPCP RAS, Chernogolovka, Russia, ⁵LPGP, Orsay, France,

⁶TU Darmstadt, Darmstadt, Germany, ⁷UCLM, Ciudad real, Spain

**n.tahir@gsi.de*

Motivation to construct the Large Hadron Collider (LHC) comes from fundamental questions of particle physics. Each of the two beams of this impressive accelerator comprises of 2808 bunches while each bunch is made of $1.15 \cdot 10^{11}$ 7 TeV/c protons. The total energy stored per beam is about 360 MJ that is sufficient to melt 500 kg of copper. Safety of operation is an extremely important issue in the presence of such powerful beams. A rapid loss of even 0.002 % of the 7 TeV/c beam at one spot could already damage a high-Z material like copper. A worst case scenario is the possibility of the full LHC beam being lost at one place. Although the probability of an accident of this magnitude is extremely small, nevertheless it is important to have full knowledge of the consequences if it ever happens. This information is essential in order to design the protection systems of the machine correctly, to set admissible risk

levels, and to determine the inventory of the spare parts needed to possibly replace the damaged equipment.

For this purpose, we carried out numerical simulations of interaction of one LHC beam with a solid copper cylindrical target. First, we calculate the energy loss by 7 TeV/c protons in copper using the FLUKA code [1], which is a fully integrated particle physics and multi-purpose Monte Carlo simulation package capable of simulating all components of the particle cascades in matter up to multi-TeV energies. This data is used as input to a 2D computer code, BIG2 [2] to simulate the hydrodynamic and thermodynamic response of the target. These simulations have shown that the LHC beam will penetrate up to 35 m in solid copper and the target material will be transformed into High Energy Density (HED) matter. This could be an additional, very important application of the LHC.

[1] A. Fasso et al., CERN-2005-10, INFN/TC-05/11, SLAC-R-773 (2005).

[2] V.E. Fortov et al., Nucl. Sci. Eng. **123** (1996), 169.

5.8 Specific features of spallation processes in a Plexiglas (PMM) under high strain rate

*¹Krasyuk I.K., ¹Geraskin A.V., ²Khishchenko K.V., ¹Pashinin P.P.,
¹Semenov A.Y., ¹Vovchenko V.I.

¹GPI, Moscow, Russia, ²JIHT RAS, Moscow, Russia

*krasyuk99@rambler.ru

Direct laser interaction and laser-driven thin foils were used for investigation spallation phenomena in a Plexiglas (PMM) targets in case of high value of strain rates. In experiments the aluminium foils with thickness 8 and 15 μm were used as impactors. The laser-driven foils mass and velocity after laser ablation and acceleration were determined by the method of their deceleration in a gas atmosphere. In experiments the 700 μm Plexiglas plates were used as the targets. On the base of experimental data we measured the position of the spallation plane and the moment at which the spall layer arrived at an additional electrocontact sensor arranged beside of rear side of target. The moment of spallation was fixed by means of piezoelectric sensor. Then, the values of spall strength and strain rate were determined by the using numerical simulations with a hydrodynamic code with a wide-range semiempirical equation of state of PMM. As a result of experiments, we found at the first

time that in case of strain rate varying from 1.5 to $6 \cdot 10^6 \text{ s}^{-1}$ the ultimate spall strength of PMM (10 kbar) was achieved. This value has been compared to a theoretical estimation.

5.9 Dense Xenon Nanoplasmas in Intense Laser Fields

¹Hilse P., ^{*2}Bornath T., ¹Moll M., ¹Schlanges M.

¹U. Greifswald, Greifswald, Germany, ²U. Rostock, Rostock, Germany

* thomas.bornath@uni-rostock.de

The interaction of intense laser fields with xenon clusters is investigated using the nanoplasma model which allows to describe different processes like ionization, heating, and expansion that occur during the laser-cluster interaction by a coupled set of hydrodynamic and rate equations.

The initial plasma in the cluster is created due to tunnel ionization described by the well-known ADK-rates. For the heating rate due to inverse bremsstrahlung, a quantum statistical expression including resonant absorption was used. Furthermore, collisions of electrons with the cluster surface are included. An important issue of laser-cluster interaction is the creation of a high-density nanoplasma. Here, the influence of correlation effects such as the lowering of the ionization energy on the ionization kinetics is of importance. Using generalized electron impact ionization rates, we found an enhancement of the yield of highly charged ions.

An effective tool to control the plasma dynamics is pulse shaping where phase and amplitude of the laser pulse are simultaneously modulated. In particular, the yield of highly charged ions can be controlled. For an understanding of the underlying physical processes in the dynamics of laser-cluster interaction, a theoretical description using a genetic algorithm and basing on the relatively simple nanoplasma model seems to be promising. In the present approach, the time evolution of the laser intensity has been parametrized. The parameters were optimized with a genetic algorithm to get, e.g, a maximal yield of a specific ion species.

The work was supported by the Deutsche Forschungsgemeinschaft, SFB 652.

5.11 Experimental investigation of femtosecond laser ablation spectral thresholds, condensed matter-dense plasma phase transition dynamics in ambient and vacuum conditions

*¹Loktionov E.Y., ²Ovchinnikov A.V., ¹Protasov Y.Y., ²Sitnikov D.S.

¹*BMSTU, Moscow, Russia*, ²*JIHT RAS, Moscow, Russia*

**stcpe@bmstu.ru*

The results of femtosecond condensed matter laser ablation opto-thermophysical and radiative gasdynamic processes experimental investigation are presented.

Laser irradiated condensed matter mass flow dynamics is an object of great interest, but is also rather difficult to be experimentally analyzed. While integral ablation rates can be obtained using several methods, data on mass flow dynamics are usually results of numerical simulations. Only two experimental time-resolved methods to investigate ablative mass flow could be rather simple to realize: high-energy photons beam probing and interference microscopy.

Using time-resolved interference microscopy (Michelson interferometer) femtosecond laser ablation spectral thresholds, mass flow integral rate and dynamics have been experimentally investigated for thin film and bulk Ti, Zr, Cu, Mo, Nb, $(CH_2O)_n$, $(C_2F_4)_n$, LiF and fused silica. Targets were irradiated by Ti:Sapphire laser ($E/S=0,1-40 \text{ J/cm}^2$ $r_0 \text{ } 20\mu\text{m}$; $\tau_{FWHM}=45 \text{ fs}$; $\lambda=266, 400, 800 \text{ nm}$) both in ambient and vacuum ($5 \cdot 10^{-4} \text{ mbar}$). Crater and near surface plasma dynamics have been investigated with 300 nm spatial and 100 fs temporal resolution. Mass flow integral rates measured are $10^{-5}-10^{-4} \text{ g/J}$. Ablation thresholds are shown to decrease for shorter wavelength irradiation.

Plume dynamics and macrostructure were analyzed using time-resolved interference (Mach-Zehnder interferometer) and shadow imaging at the same conditions and simultaneously with interference microscopy. Transient density distribution, shockwave ($10^3 - 10^5 \text{ m/s}$) and plume velocities have been obtained. Plume average temperature and composition were estimated from emission spectra.

Crater and plume dynamics interconnection is considered and advantages of complex experimental analysis are discussed. Femtosecond laser ablation performance for different target materials, irradiation wavelengths and ambient conditions is analysed. Presented results are discussed and compared with nanosecond laser ablation.

5.17 Non Linear propagation of intense laser beams through collisional plasmas

*Walia K., Singh A.

NIT Jalandhar, Jalandhar, India

**keshavpaulwalia@gmail.com*

In the present paper, Non-linear propagation of intense laser beams through collisional plasma is studied by moment theory approach. As a result of it self focusing happens. Effect of change in absorption coefficient and plasma density on beam width parameter is also analyzed. It is observed from the analysis that increasing the plasma density decreases focusing length due to increase in non-linear part of dielectric constant. Also, due to increase in absorption coefficient, extent of self focusing decreases. This is due to decrease in energy of beam which is equivalent to weakening of non linearity effect.

6 Dense astrophysical plasmas

6.4 Low-velocity ion stopping in binary ionic mixtures

*²Fromy P., ²Deutsch C., ¹Tashev B.A., ¹Baimbetov F.B.

¹*IETP KazNU, Almaty, Kazakhstan, ²Paris Sud, Orsay, France*

* *tba81@mail.ru*

Stopping power of thre component plasmas contains carbon an ferrum ions are developed.

7 Phase transitions in plasmas and fluids

7.1 Fluctuation approach to the nonideal plasma equation of state calculation.

*Saitov I.M., Lankin A.V., Norman G.E.

JIHT RAS, Moscow, Russia

**saitov_06@mail.ru*

The nonideal plasma equation of state is studied in the frames of the fluctuation approach which provides the self-consistent joint description of free and weakly bound electron states in equilibrium plasmas is presented [1]. The approach avoids a certain peculiarity of the chemical model for which at calculation of value of free energy the account of dependence of the statistical sums $Q_i(T, \varepsilon(\{n_j\}, T))$ from the thermodynamic parameters expressed through variable border of trimming of a spectrum of free particles $\varepsilon(n, T)$ is necessary. Direct result of the account of the given dependence is occurrence of additional corrections to all thermodynamic quantities containing derivatives $\partial Q_i(T, \varepsilon(\{n_j\}, T)) / \partial \varepsilon$ [2].

The molecular dynamics method is used. The electron-ion interaction is described by the density- and temperature-independent cutoff Coulomb potential. The range of nonideality parameter $\Gamma = 0.1 \div 2$ is studied. In this region of parameters of nonideality there is an instability, which is characterized according to circular approach by positive value of a derivative of pressure on volume owing to what it is possible to assume occurrence of diphasic area [3].

At the analysis of fluctuations of pressure the region of values of Γ in which appreciable difference of function of distribution of pressure from normal distribution is observed has been revealed, and the received results can be approximated by superposition of two Gauss distribution functions. The given fact could be considered as an indirect conformation of existence of diphasic area.

Both single and multiply ionized plasmas are considered.

- [1] A.V. Lankin, G.E. Norman. Journal of Physics A: Mathematical and Theoretical **42** (2009).
- [2] V.K. Gryaznov, I.L. Iosilevskiy. Encyclopaedia of low temperature plasma. /Ed. by V.E. Fortov, M.: Fizmatlit, 2004. 170.
- [3] G.E. Norman, A.N. Starostin. High Temperature **6** (1968). 394.

7.3 Sound velocity measurements behind the shock wave in tin

Zhernokletov M.V.

*RFNC-VNIIEF, Sarov, Russia
root@gdd.vniief.ru*

In the pressure range of 30 – 138 GPa by optical method and the method of manganin gauges the sound velocity in shock-compressed tin was measured. The comparison of experimental data and the calculations was conducted. The tin melting range on the principal Hugoniot (60 – 85) GPa was found.

7.5 The Investigation of Phase Changes in Cerium and Titanium by PVDF-gauges

²**Borisenok V.A.**, ^{*2}**Zhernokletov M.V.**, ²**Simakov V.G.**,
¹**Zocher M.A.**, ¹**Cherne F.J.**

¹*LANL, Los Alamos, USA*, ²*RFNC-VNIIEF, Sarov, Russia*
**root@gdd.vniief.ru*

The phase transitions in shock-compressed samples of cerium and titanium with PVDF-gauges were investigated. In the pressure range of $4 \leq P < 12$ GPa in cerium a double-wave structure, consisting of head compression wave and the following shock-wave was registered. Such a structure is formed in cerium as a result of isomorphic (γ - α) phase transition. The analysis of shock wave structure and rarefaction shock in the diapason of (0.6:3.0) GPa proves that in cerium a rarefaction shock wave is formed in the release phase. In titanium, at the loading pressure of ≈ 21 GPa on the plastic wave profile an anomaly at the pressure of 11.5 GPa, which is associated with the phase $\alpha \rightarrow \omega$ transformation is found out.

Index

- Adams J., 25
Amirov R.H., 11
Apfelbaum E.M., 26
- Baimbetov F.B., 14, 43
Balzer K., 30
Bauch S., 30
Beisinboeva H., 36
Berdierov G., 9
Bonitz M., 10, 30
Borisenok V.A., 45
Boriskov G.V., 21
Bornath T., 40
Budnik A.P., 7
Bykov A.I., 21
- Cherne F.J., 45
Ciftja O., 10
- Dejonghe G., 19
Deputatova L.V., 7
Deutsch C., 38, 43
Dufty J.W., 10
Dutta S., 10
- Egorov N.I., 21
- Faenov A.Ya., 31
Filinov A.V., 10
Fortov V.E., 7, 20, 34, 38
Fromy P., 43
- Gagarin S.V., 31
Geraskin A.A., 12
Geraskin A.V., 39
Gericke D.O., 37
Grinenko A., 37
Gryaznov V.K., 25, 34
- Hilse P., 40
Hochstuhl D., 30
Hoffmann D.H.H., 38
- Ignjatovic Lj.M., 32
Iosilevskiy I.L., 23, 34
Ivanov D.S., 15
- Karakhtanov V.S., 33
Khaydarov R., 9, 36
Khishchenko K.V., 12, 22, 39
Kholboev A., 36
Khomkin A.L., 32
Khrapak A.G., 20
Kislenko S.A., 11
Kosarev V.A., 7
Kozlov A.I., 31
Krasyuk I.K., 12, 39
Kudyshev Z.A., 14
Kuropatkin Yu.P., 21
Kvitov S.V., 34
- Lankin A.V., 27, 44
Loboda P.A., 19, 31
Loktionov E.Y., 41
Lomonosov I.V., 38
Lorenzen S., 27
Luk'yanov N.B., 21
Lyubartsev A.P., 8
- Magunov A.I., 31
Mihajlov A.A., 32
Minkova N.R., 13
Mintsev V.B., 25
Mirabotalebi S., 13
Mironenko V.D., 21
Moll M., 40
Molodets A.M., 20

Morozov S.V., 31
Nikolaev D.N., 34
Norman G.E., 44
Omarbakiyeva Y.A., 18
Osmani O., 15
Ovchinnikov A.V., 41
Pain J.C., 19
Pashinin P.P., 12, 39
Pavlov V.N., 21
Pikuz T.A., 31
Piriz A.R., 38
Polyakov E.A., 8
Popova V.V., 19, 31
Protasov Y.Y., 41
Pyalling A.A., 34
Röpke G., 18, 25, 27, 28, 33
Rajae L., 13
Ramazanov T.S., 18
Redmer R., 25, 33
Reinholz H., 25, 27, 33
Rethfeld B., 15
Rykov V.A., 7
Saitov I.M., 44
Sakan N.M., 32
Samoylov I.S., 11
Schlanges M., 40
Schmidt R., 38
Semenov A.Y., 12, 39
Shadrin A.A., 19
Shakhray D.V., 20
Shemyakin O.P., 22
Shilkin N.S., 25
Shumikhin A.S., 32
Shutov A., 38
Simakov V.G., 45
Singh A., 38, 42
Sitnikov D.S., 41
Skobelev I.Yu., 31
Sperling P., 28
Sreckovic V.A., 32
Tahir N.A., 38
Tashev B.A., 43
Ternovoi V.Ya., 34
Urnov A.M., 31
Vainshtein L.A., 31
Vanina I.A., 31
Varentsov D., 37
Vladimirov V.I., 7
Vorberger J., 37
Vorontsov-Velyaminov P.N., 8
Vovchenko V.I., 12, 39
Voznesenskiy M.A., 8
Walia K., 38, 42
Wierling A., 27, 28
Winkel M., 28
Yakub E.S., 16
Yakub L.N., 16
Zhernokletov M.V., 45
Zocher M.A., 45